Contour-Net
A Model for Tactile Contour-tracing and Shape-recognition

André Frank Krause[1], Thierry Hoinville[1,2], Nalin Harischandra[1] and Volker Dürr[1,2]
[1]*Department of Biological Cybernetics, Bielefeld University, Bielefeld, Germany*
[2]*Cognitive Interaction Technology - Centre of Excellence (CITEC), Bielefeld University, Bielefeld, Germany*

Keywords: Tactile Sensor, Contour Tracing, Shape Recognition, Artificial Neural Network.

Abstract: We propose Contour-Net as a bio-inspired model for rhythmic movement control of a pair of insectoid feelers, able to successively sample the contour of arbitrarily shaped objects. Initial object contact initiates a smooth transition from a large-amplitude, low-frequency searching behaviour to a local, small-amplitude and high-frequency sampling behaviour. Both behavioural states are defined by the parameters of a Hopf Oscillator. Subsequent contact signals trigger a 180° phase-forwarding of the oscillator, resulting in repeated sampling of the object. The local sampling behaviour effectively serves as a contour-tracing method with high robustness, even for complicated shapes. Collected contour data points can be directly fed into an artificial neural network to classify the shape of an object. Given a sufficiently large training dataset, tactile shape recognition can be achieved in a position-, orientation- and size-invariant manner. Only minimal pre-processing (normalisation) of contour data points is required.

1 INTRODUCTION

The tactile sense enables humans and animals to actively perceive their immediate surrounding through direct physical contacts with an object (Lee and Nicholls, 1999). In contrast to vision, direct tactile sampling of an object allows to 'feel' object properties like surface texture, chemical properties, temperature, compliance and humidity, that are hard to obtain otherwise (Lederman and Klatzky, 2009). The sense of touch is independent of light conditions, and works equally well night and day. Moreover, the direct contact with an external object yields reliable distance information (Patanè et al., 2012). Therefore, the tactile sense plays an important role throughout the animal kingdom, especially in nocturnal species.

Several insect species, for example the honey bee (*Apis mellifera*), the American cockroach (*Periplaneta americana*) and the Indian stick insect (*Carausius morosus*) have become important model organisms for the study of the sense of touch. Insects carry a pair of antennae that are densely covered with sensory hairs of different modalities (Staudacher et al., 2005). Honeybees, for example, show a high concentration of tactile hairs at their antennal tip (Esslen and Kaissling, 1976). Active tactile scanning of surfaces allows them to discriminate the micro texture of flowers (Kevan and Lane, 1985) or artificial gratings (Erber et al., 1998).

An important constraint of the insect tactile system is that antennae essentially are one-dimensional structures that are incapable of providing a two-dimensional image "at a glance". Instead, antennae need to be moved actively in order to sample information from different locations within their working-range. Active tactile sensing is of particular relevance in near-range exploration. Many insects actively use their antennae for obstacle localization, orientation behaviour, pattern recognition, and even for communication (Staudacher et al., 2005). Similarly, mammals like cats or rats use active whisker movements to detect and scan objects in the vicinity of the body.

Insect antennae and mammal whiskers have inspired robotic research in the area of tactile sensors. Early work by Kaneko et al. (1998) describes an artificial antenna using a flexible beam capable of detecting 3D contact locations and surface properties. Russell and Wijaya (2003) applied an array of whiskers that passively scan over an object to recognize its shape using advanced pre-processing contact-points and decision trees. In Solomon and Hartmann (2006), robotic whisker arrays were used to generate 3D spatial representations of the environment and extract object shapes. Related work done by Kim and Möller

Frank Krause A., Hoinville T., Harischandra N. and Dürr V..
Contour-Net - A Model for Tactile Contour-tracing and Shape-recognition.
DOI: 10.5220/0004821700920101
In *Proceedings of the 6th International Conference on Agents and Artificial Intelligence* (ICAART-2014), pages 92-101
ISBN: 978-989-758-016-1

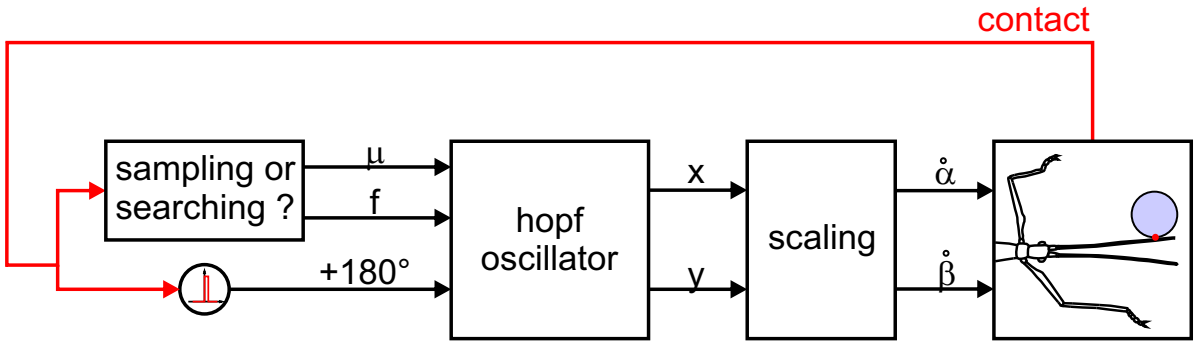

Figure 1: Block diagram of Contour-Net. The binary contact signal (red) determines the frequency and amplitude of the Hopf Oscillator. The discrete impulse block guarantees that the oscillator phase is forwarded once by 180°, resulting in a movement away from the object surface. The output of the oscillator is then scaled and drives a simulated or real robot antenna using velocity control of antennal joints.

(2007) used a vertical whisker array to detect the vertical shape and curvature of objects.

Stick insects continuously and rhythmically move their antennae during locomotion (Dürr et al., 2001) and during tactile probing of external objects (Krause et al., 2013b). Upon antennal contact with an obstacle, stick insects modulate both the frequency and the amplitude of the rhythmic antennal movement, affecting both antennal joints in a context-dependent manner (Schütz and Dürr, 2011; Krause and Dürr, 2012). For example, when climbing a square obstacle, they show a contact-induced switch in behaviour from a broad, almost elliptical searching pattern to a local sampling pattern with higher frequency and lower amplitude (Krause and Dürr, 2012). This switch to a local sampling strategy may be interpreted as an effort to gather more detailed spatial information close to previous touch locations, effectively leading to the sampling of an obstacle's contour.

A fundamental concept explaining such rhythmic movements in vertebrates and invertebrates is the central pattern generator (CPG, for a review see Ijspeert (2008)). The CPG activity is often modulated by sensory input, proprioceptive input and descending signals from higher level brain centres. Antennal movements in stick insects are assumed to be driven by CPGs, because rhythmic activity can be evoked pharmacologically (Krause et al., 2013b).

Here, we present a simple but effective, bio-inspired, CPG-based model capturing the essence of tactile sampling in stick insects. The model is able to trace the contour of an obstacle using an actively movable tactile probe. The CPG activity is modulated by a single, binary sensor signal: if the tactile probe is in contact with the obstacle or not.

2 CONTOUR-NET

The contour-tracing model presented here was coined *Contour-Net*, hinting at its possible integration into existing, modular architectures for simulation and control of hexapod walking (*Walknet*, Schilling et al. (2013)) and ant-inspired navigation (*Navi-Net*, Hoinville et al. (2012)). The model captures the essential characteristics of antennal tactile sampling in stick insects: rhythmic searching movements using an antenna with two revolute joints with strong coupling and a contact-triggered switch to local sampling. Such rhythmic movements can be obtained as limit cycles of nonlinear dynamical systems, typically systems of coupled nonlinear oscillators. In our case the optimal choice is a "Hopf Oscillator", because the two state variables of the oscillator exhibit a fixed phase coupling and can directly drive the two joints of an antenna.

2.1 Hopf Oscillator

The Hopf Oscillator is a dynamical system defined in Cartesian Space by the following differential equations:

$$\dot{x} = \gamma\left(\mu^2 - r^2\right)x - \omega y$$
$$\dot{y} = \gamma\left(\mu^2 - r^2\right)y + \omega x$$

with $r = \sqrt{x^2 + y^2}$. The amplitude of the oscillator converges to μ, with γ defining the speed of convergence and ω setting the frequency of the limit cycle. Further, the phase of the oscillator can be set with $x = \cos(\varphi), y = \sin(\varphi)$.

The Hopf Oscillator has several advantages: First, it has a stable limit cycle behavior (i.e., perturbations decay quickly) with a fixed, non-drifting, 90° phase relationship between the x and y components

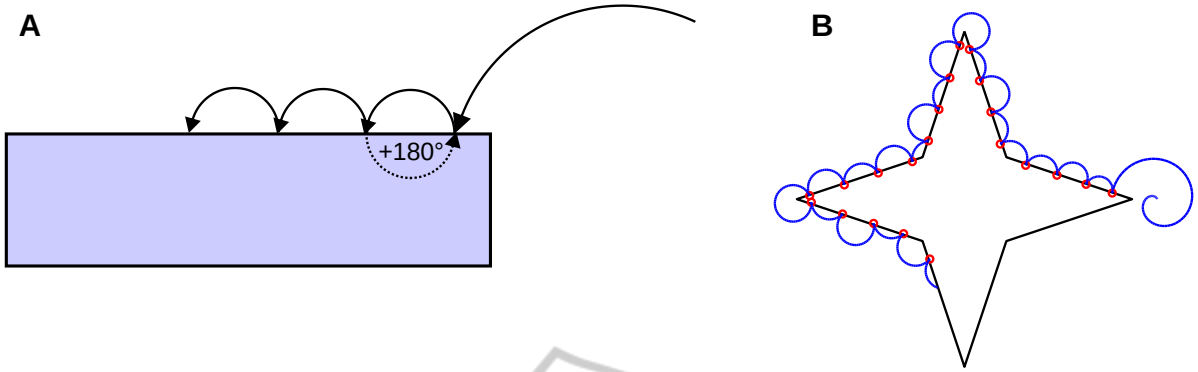

Figure 2: **A**: Core idea of Contour-Net. Each contact induces a 180° phase forwarding of a circular movement. Combined with velocity control of a tactile probe, the resulting change in movement velocity and direction causes the probe to "bounce off" the surface at every contact event, resulting in a successive scan along the object's shape. **B**: 2D simulation of contact-triggered contour tracing. *Black*: star-shaped object. *Blue*: trajectory of the antennal tip. *Red dots*: contact locations.

of the oscillator. Second, it is simple and well defined in terms of amplitude, phase and frequency, which can be adjusted independently from each other. Because of these properties, smooth online modulation of trajectories can be achieved through changing parameters of the system at run-time. Moreover, these properties help in entrainment of the CPG rhythm through sensory feedback, e.g., when being coupled with a mechanical system (Righetti and Ijspeert, 2006). Hopf CPG's have been applied successfully to biped (Buchli et al., 2005; Righetti and Ijspeert, 2006) and quadruped (Brambilla et al., 2006; Ijspeert et al., 2007) locomotion.

2.2 Contact-triggered Contour Tracing

The basic idea of the contour-tracing model, as illustrated in figure 2A, is that each contact event triggers a phase shift in the cyclic sampling movement of the antenna. Ideally, this phase shift should cause the antenna to "bounce off" the object after each contact. Using a Hopf Oscillator to control the antennal position directly would require memorizing the location of the centre of oscillation, and shifting it along the object surface. The need for a memory structure can be avoided if the Hopf Oscillator output is used to set the antennal velocity rather than position. Figure 2B shows the "scan path" (in analogy to eye-tracking scan paths) along a star-shaped 2D-object. The velocity commands applied to the antennal joints, α and β are given by:

$$\Delta\alpha = s_1 x$$
$$\Delta\beta = s_2 y$$

where s_1 and s_2 are scaling factors, setting the maximum action range of the antenna. Setting these factors to distinct values leads to ellipsoid trajectories as found in stick insect antennal movements (Krause and Dürr, 2004).

The 2D simulation shown in figure 2B was implemented in Matlab and contact locations are calculated using the Geom2D toolbox (http://matgeom.sourceforge.net).The simulated antenna and the Hopf Oscillator equations are iterated using first order, forward Euler Integration with a fixed time step Δt.

After a contact is detected by the antenna, the amplitude μ and the frequency ω are immediately switched from a large amplitude, low frequency "searching mode" to a high-frequency, low amplitude "sampling mode". Once a certain time span $T_{sampling}$ has passed without encountering a further contact event, the parameters are switched back to the "searching mode" pattern.

A 180° phase shift can be easily implemented by negating the Hopf Oscillator state variables: $x_{t+1} = -x_t$ and $y_{t+1} = -y_t$. Because of the discrete-time nature of numerical simulations, contacts with an obstacle may last longer than a single time step. Therefore, the 180° phase shift should be applied only once for each contact event. In the block diagram in figure 1, this is indicated by the discrete pulse block.

2.3 Robustness Evaluation

The robustness of the contour tracing algorithm was evaluated by scanning a rough surface. For generation of a random contour, we tested shapes with linear segments of random orientation and length. The goal for the algorithm was to completely scan the surface from the right to the left outermost side without getting stuck, see figure 3A for a sample surface. The surface was structured as a 10 units long, initially straight line with 40 uniform segments. The locations (x_i, y_i) of the nodes connecting the segments were

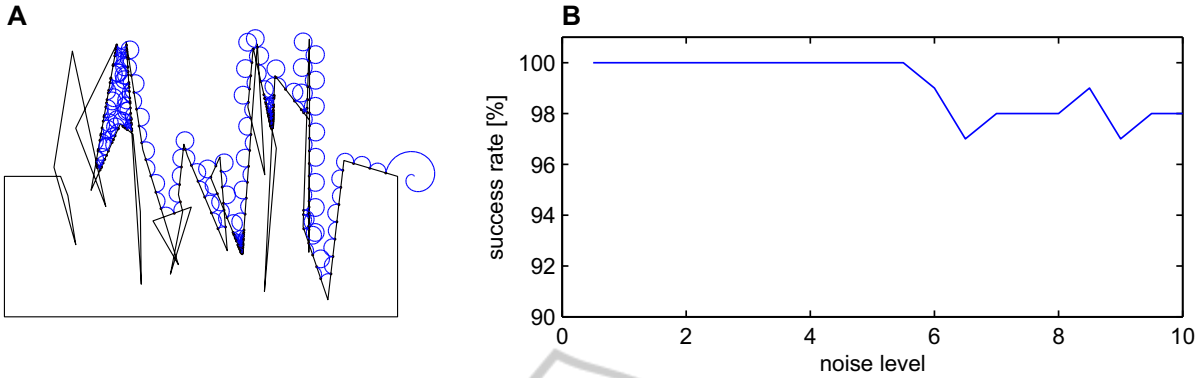

Figure 3: Robustness evaluation of the contour-tracing algorithm. **A**: Extreme example, in which the antenna got trapped in a cavity of the random contour. **B**: Success rate of contour-tracing in percentage. N=100 trials.

Table 1: Simulation parameters.

parameters	2D-Sim	3D-Sim
γ	4.0	4.0
$\mu_{searching}$	1.0	0.5
$\mu_{sampling}$	0.2	0.1
$\omega_{searching}$	1.0	1.0
$\omega_{sampling}$	2.0	2.0
Δt	0.02	0.02
$s_1 = s_2$	1.0	0.5

then randomized by $x_i = x_i + 0.15 * rand(-r,r)$ and $y_i = y_i + rand(-r,r)$ where $rand(-r,r)$ generates uniformly distributed random numbers between $-r$ and r. N=100 trials were performed for each noise level $r = 0.5, 1, .., 10$. In almost all trials, the rough surface could be completely scanned from start to end. Figure 3A shows one of the rare cases, where the contour tracing algorithm got trapped in a cavity. Figure 3B shows the overall success rate, i.e. the percentage of trials that completely scanned the rough surface.

2.4 3D Simulation

The contour tracing algorithm also works reliably in 3D space. Virtually no change in the algorithm is required, except minor parameter tuning, see table 1. Figure 4 shows a kinematic antennal model with orthogonal joint axes (similar to a cardan joint), probing several complex objects like a Torus or a Octahedron. Contact events were calculated using the Geom3D Matlab package, including the contact distance along the tactile probe.

3 TACTILE SHAPE RECOGNITION

An application scenario for Contour-Net is tactile shape recognition of sampled objects. Each contact point with the surface can deliver direct information about the contact distance, the current joint angles at contact time and indirect values like the state of the Hopf Oscillator. Collecting these values should allow a discrimination of object shapes based on previous learned examples. Here, we apply a plain but large feed-forward neural network to solve the classification task. Previous results have shown that multilayer neural networks can classify hand-written digits and temporal eye-tracking data with minimal preprocessing, only (Krause et al., 2013a). We propose to feed the collected and normalised contact-point data directly as input values to the network. Normalisation rescales the different data components to a range from $[-1,1]$.

Due to the well known *curse of dimensionality* problem (shrinking norm, Beyer et al. (1999)), the training dataset should be as large as possible, requiring long training times with common neural network training algorithms. For example, standard backpropagation has to deal with local minima (LeCun et al., 1998) and vanishing gradients (Hochreiter et al., 2001). Using No-Prop-*fast* (Krause et al., 2013a), a special case of an Extreme Learning Machine (Huang et al., 2006), these problems can be circumvented and almost interactive training times can be achieved. This allows the generation of parameter tuning curves with many repetitions of the learning process using personal computers.

3.1 Training Dataset

To collect a large training dataset, four different 2D-shapes (triangle, square, star, circle) were traced using Contour-Net. The shape size was scaled between 100% and 200%, shapes were rotated randomly between 0° and 360°, and the initial contact location was also randomized. Figure 6 shows a small sample from

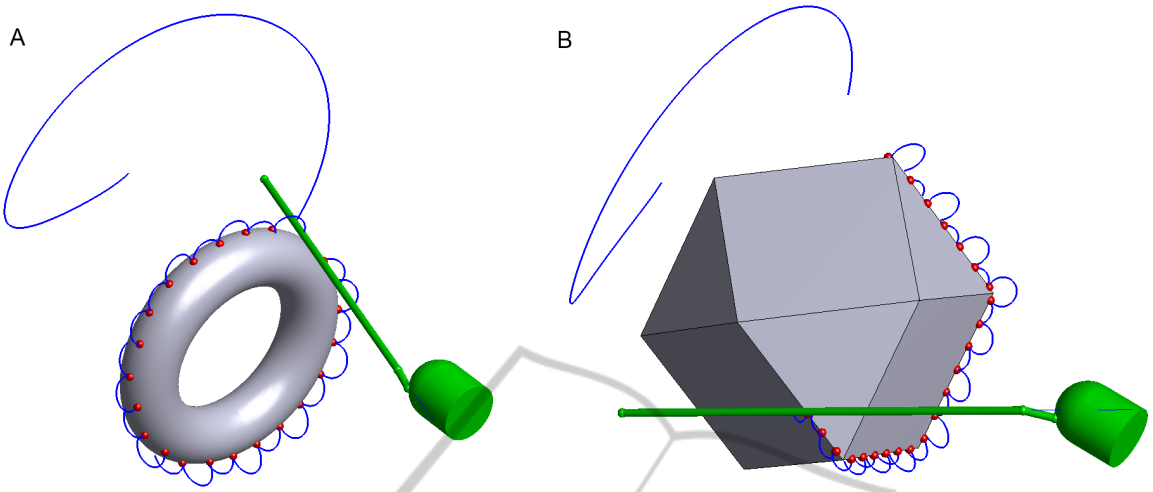

Figure 4: 3D simulation of contact triggered contour tracing. Grey: objects. Green: insect head with left antenna. Blue: trajectory of the antennal tip. Red dots: contact locations. **A**: torus, **B**: octahedron.

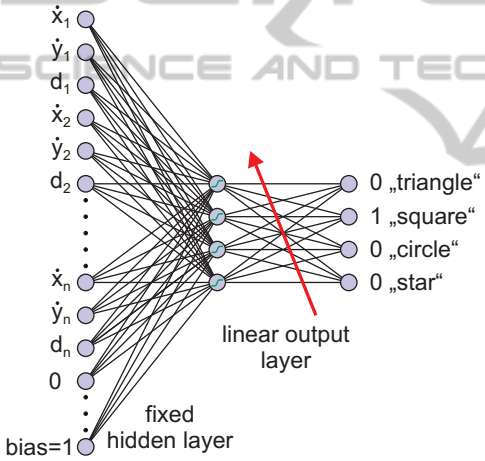

Figure 5: General network structure used for shape recognition. A plain feed forward network with a large hidden layer is used. Data components ($\dot{x}$, $\dot{y}$ from Hopf Oscillator, contact distance d along antenna) collected during a contour-sampling are serialized, rescaled to the range -1 to 1 and fed into the network. Shorter contour-scans can be zero-padded. Hidden layer weight values are initialized randomly and only the output layer is trained (see text). Class labels use a “one-out-of-n” coding.

the 2D-dataset. A fixed number of contact points was selected such that all shapes in all sizes were ’encircled’ at least once, hence completely traced. 400 random samples with 35 contact points per shape were collected, resulting in a training dataset with 1600 samples. Each contact point consisted of 3 components: the $\dot{x}$ and $\dot{y}$ velocity components of the Hopf Oscillator and the object size. Hence, the raw input to the neural network has 105 dimensions. The network has one hidden layer and 4 outputs. Output values use a “one-out-of-n” coding scheme. The hidden layer of No-Prop networks (Widrow et al., 2013) is fixed and was initialized with uniformly distributed random numbers. Figure 5 shows the general network structure.

3.2 Classification Performance

25 randomly initialized networks were trained on the dataset, and performance was evaluated using 10-fold cross validation. Figure 7B shows how the classification accuracy depends on the hidden layer size. As shown in Krause et al. (2013a), essentially two components influence the performance: the hidden layer size and the hidden layer weight range. The optimal weight range of hidden layer units does not depend on the number of hidden layer units (figure 8) but on the number of inputs and was estimated to be from -0.5 to 0.5 for both the 2D and 3D training dataset (see section 3.3). Figure 7B (blue curve) shows that an acceptable, size- and rotation-invariant shape classification can be achieved. The discrimination rate peaks around 600 hidden units and decreases after that. The low spread of performance values indicates that the algorithm has not to deal with local minima. This is a favourable feature of the No-Prop method, see also Widrow et al. (2013).

Yet, contour tracing trajectories were found to be fairly variable, depending on angle of attack of the tactile probe relative to the surface. Figure 7A shows an example where the probe arrives at a flat angle to the surface. The subsequent, contact-induced 180° phase shift of the oscillator causes the probe to leave the surface in a suboptimal, backward direction. The resulting pattern alternates between a flat and large arc.

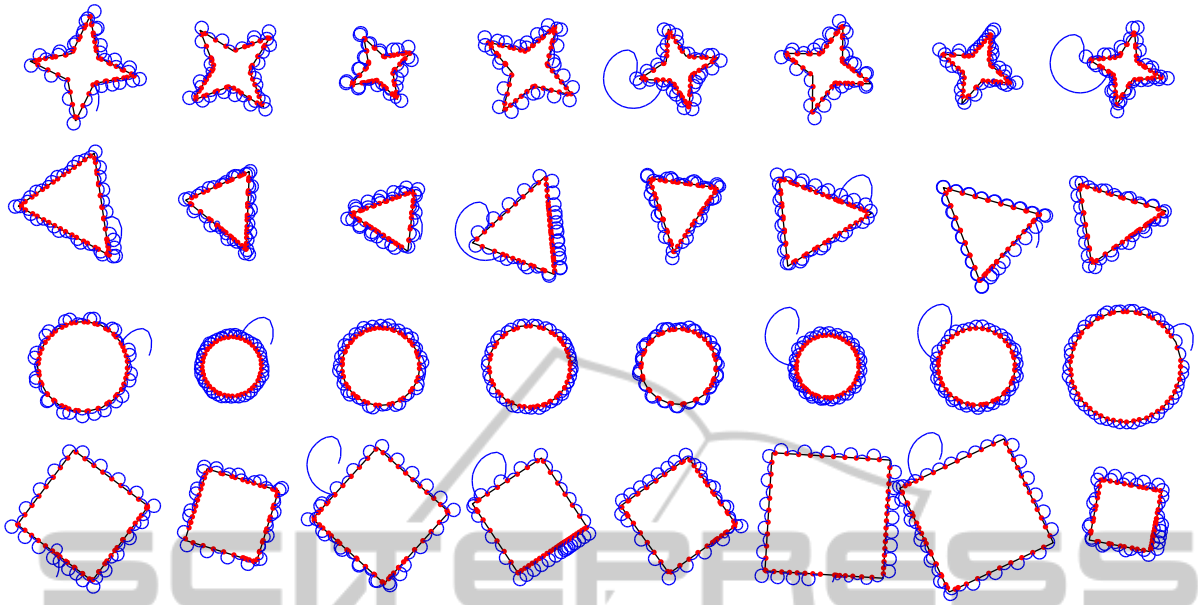

Figure 6: Sample collection of the four different shapes used for the classification task. The size and orientation of the shapes as well as the initial contact location was randomized.

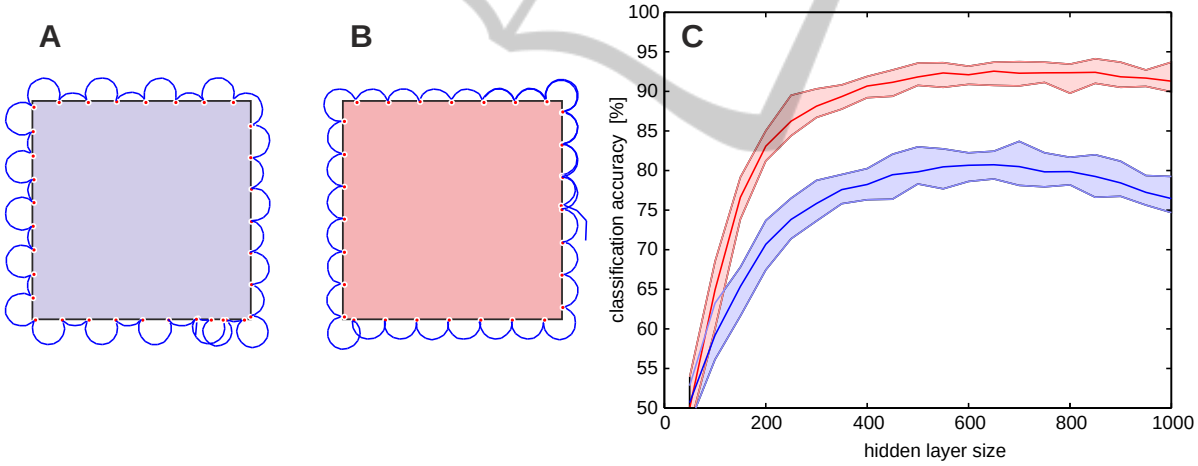

Figure 7: Classification results improve after incorporating surface-normal information into Contour-Net. **A**: Sampling trajectory using a fixed 180° phase shift of the Hopf Oscillator after contact. **B**: The phase of the oscillator is set such that the tactile probe leaves the object surface in the normal direction after a contact. The resulting sampling trajectory is more regular. **C**: Classification accuracy using a fixed phase shift (blue), and variable phase shift depending on the object surface normal (red). A training dataset with four shapes as shown in figure 6 with n=400 samples per shape was used. N=25 repetitions. Solid curve = mean value, shaded area = min and max values.

Approaching a surface perpendicular with an optimal, 90° angle, not only avoids potential slip, see Kaneko et al. (1995). Improving the regularity of the scan path might also improve the shape classification performance. A simple solution would be to use the estimated surface normal [1] for setting the outgoing angle after contact. Figure 7B shows an example of an improved sampling trajectory. The main advantage for the classificator is a lower spread of contact parameters along flat regions of an object and a more pronounced change in values at sharp edges. This is reflected in more than 10% improvement of the classification accuracy. Figure 7C, red curve, shows the im-

[1] In the simulation, the surface normal was estimated by a local, 360° subsampling of the surface around the contact position. From the resulting list of intersections with the object, an average surface normal vector could be calculated similar to the mean resultant vector in circular statistics.

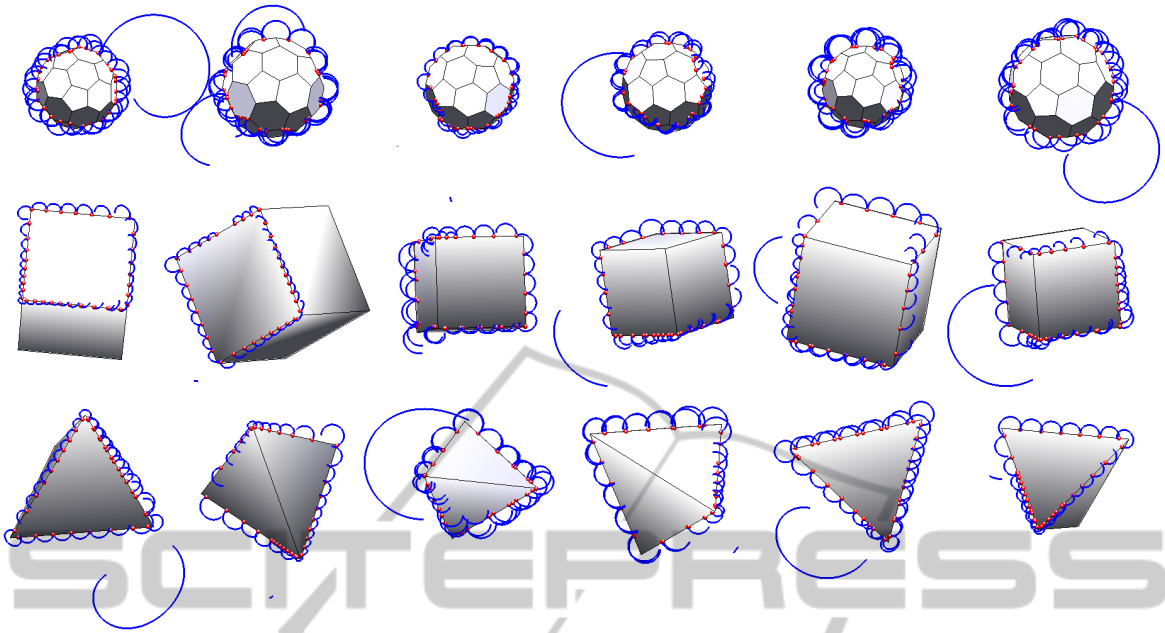

Figure 9: Sample collection of three different 3D objects: 1. row: soccer ball; 2. row: cube; 3. row: tetrahedron. The size, position and spatial orientation of the shapes as well as the initial antennal location were randomized.

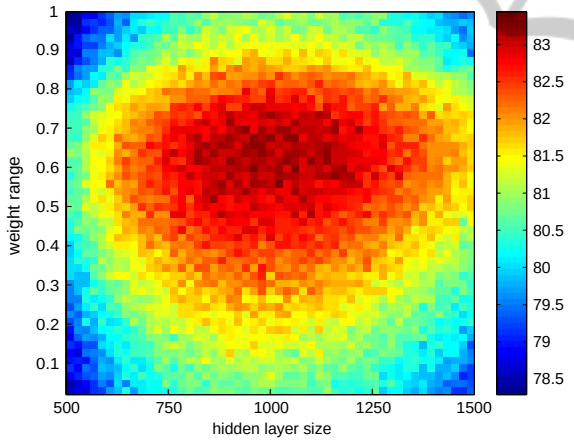

Figure 8: Classification accuracy (color coded) depending on weight range and hidden layer size. Used training dataset: 3D shapes, n=1000 samples per shape, n=20 repetitions. The optimal weight range value is independent from the hidden layer size.

proved recognition rate using a dataset identical in parameters to section 3.2, but generated using ContourNet with variable phase shift depending on the surface normal.

3.3 3D Shape Classification

Subsequently, classification performance using 3D objects was tested. Three different objects were used: a soccer ball, a cube and a tetrahedron, see figure 9. The objects were scaled between 100% and 150%; placed at a random position $(x,y,z) = [20..30,-5..5,-5..5]$ in front of the antenna; and rotated randomly around all axes in the full range of 360°. The initial antennal location around the object was also randomized. Three datasets with 400, 1000 and 3000 random samples per shape with 35 contact points per shape were collected. From each contact event, three components were used: the $\dot{x}$ and $\dot{y}$ values of the Hopf Oscillator and the contact distance along the antenna. The neural network had 105 inputs and three outputs.

Figure 10 shows the classification accuracy for the three differently sized datasets. The increased complexity of the task required a very large dataset to achieve a classification rate above 90%. Due to the random rotation around all axes, the supervised learning algorithm has to be trained on a sufficiently large number of contour projections of the objects. Restricting the task to a fixed object size and to a random rotation around a single axis, only, would certainly reduce the necessary size of the training dataset. Figure 10B shows that the contact distance information only slightly improved classification performance by 5%. Hence, the contact distance along the antenna is not essential and does not need to be very precise or may be omitted completely.

3.4 Performance Evaluation

The No-Prop-*fast* method was compared with two

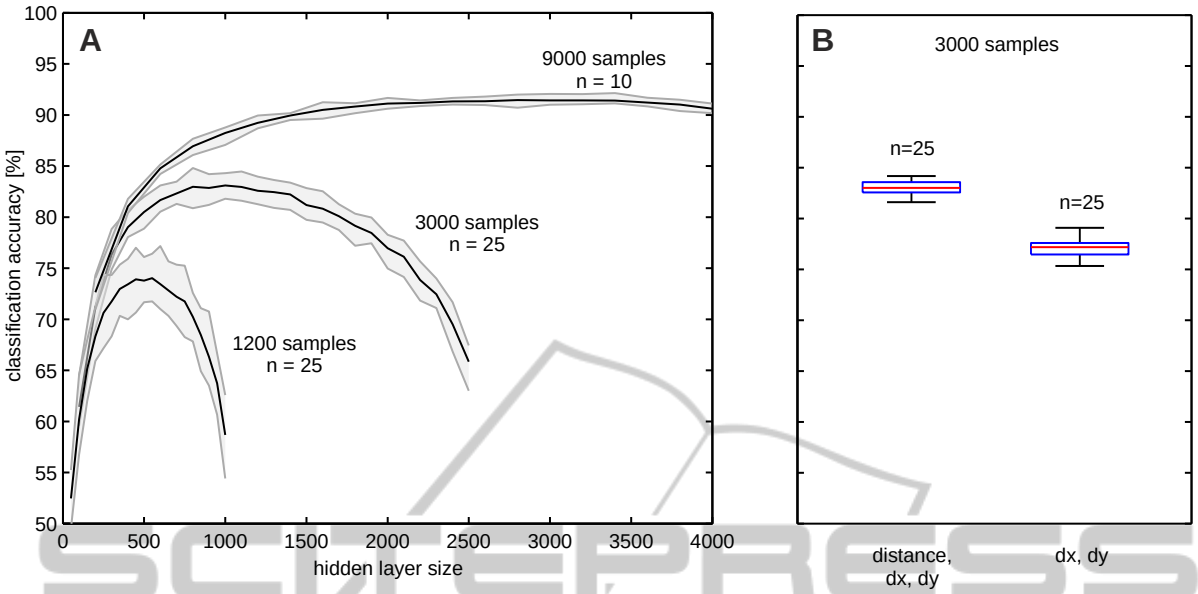

Figure 10: 3D shape classification performance strongly depends on the sample size. **A**: Performance for three different sample sizes. The neural network requires a fairly large sample size to achieve high performance. It needs to "see" several contour projections of the randomly oriented objects. **B**: Influence of the input components on performance. Performance is still good with the velocity components of the Hopf Oscillator, only.

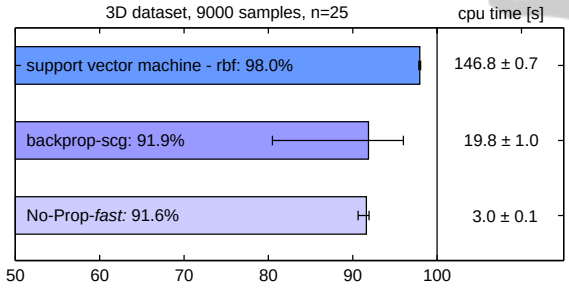

Figure 11: Classification accuracy and training times of three different algorithms. First row: No-Prop-*fast* ($n_{hidden} = 3000$), second row: scaled conjugate gradients backpropagation ($n_{hidden} = 64$), third row: gaussian kernel support vector machine. Bars show median, whiskers show min and max values, CPU times are given as mean±SD.

other algorithms, the default pattern classification algorithm of the Matlab 2012a neural network toolbox, scaled conjugate gradient backpropagation (BP_{scg}) and an implementation of a gaussian kernel support vector machine (SVM_{rbf}) found in the Matlab 2012a statistics toolbox. Figure 11 shows recognition rates and CPU times of these algorithms, applied to the 3D shape dataset with 9000 patterns. CPU time measurements were performed on a Dell Precision T3500 Workstation (Intel Xeon W3530 CPU at 2.8 GHz with 8 Mbyte second level cache) running Windows 7. The three different algorithms were evaluated using ten-fold cross-validation and 25 repetitions with randomized samples and randomly initialized networks.

A separate SVM_{rbf} was trained for each shape (one-against-all classification), using the matlab function 'svmtrain' with $sigma\_rbf = 4.2$ and $boxconstraint = 10$. All other parameters were kept at their default values. The performance of BP_{scg} was tested using a feedforward network with a single hidden layer (64 units), created with the Matlab function 'patternnet' and trained with all parameters at their default values. SVM_{rbf} achieved the highest median recognition rate (98%). Recognition rates of BP_{scg} were lower (92%) with high spread, but individual networks achieved up to 96%. No-Prop-*fast* follows with 91%.

While the recognition rates of all three algorithms are above 90%, training times were found to differ significantly. Values given in figure 11 show the average duration of individual training runs (n=250). The Matlab implementation of SVM_{rbf} required almost 147 seconds to learn the dataset, while No-Prop-*fast* required only three seconds. Hence, for the shape recognition task, No-Prop-*fast* is approximately 50 times faster than SVM_{rbf} and still six times faster than the Matlab implementation of one of the fastest BP-algorithms.

4 CONCLUSIONS

Contour-Net is a robust, bio-inspired method for tactile contour-tracing. In its simplest instantiation, it

requires only a single, binary signal: if the antenna or tactile sensor is in contact with an object or not. Yet, the model captures essential behaviours observed in its natural paragon, the stick insect antenna (Dürr et al., 2001). For example, it implements the contact-induced switch from a large amplitude searching behaviour to a local, higher frequency sampling of an object (Krause et al., 2013b). Contour-Net can be easily extended to use two or more antennae including mutual coordination and attentive visual target tracking, as will be shown in a follow-up paper.

Raw, minimally pre-processed (normalisation) data collected from contact events was sufficient to achieve rotation-, size- and position- invariant shape recognition rates of over 90% using a plain feed-forward neural network. A drawback for robotic applications is that the training dataset needs to be fairly large. Instead of using raw data as the network input, extracting higher level features from collected contour points should significantly reduce the required amount of training samples. Possible features might be the average Euclidean distance and the spread of Hopf Oscillator phase differences between successive contact points. An unsupervised learning algorithm (SOM; Boltzmann Machine) will be closer to natural, continuous learning (automatic clustering with delayed categorization).

We have further shown that incorporating surface normal information will improve not only the regularity of the sampling trajectory, but also improve the recognition performance of a neural network. Hitting a surface perpendicular can potentially reduce slip of an insect antenna inspired robotic tactile sensor (Kaneko et al., 1995). The reliable and fast detection of the surface normal using a tactile sensor will be a challenging and interesting task.

ACKNOWLEDGEMENTS

This work was supported by EU grant EMICAB (FP7-ICT, grant no. 270182) to Prof. Volker Dürr. We thank Prof. Holk Cruse for valuable comments on earlier versions of the manuscript.

REFERENCES

Beyer, K., Goldstein, J., Ramakrishnan, R., and Shaft, U. (1999). When is "nearest neighbor" meaningful? In Beeri, C. and Buneman, P., editors, *Database Theory - ICDT 99*, volume 1540 of *Lecture Notes in Computer Science*, pages 217–235. Springer Berlin Heidelberg.

Brambilla, G., Buchli, J., and Ijspeert, A. (2006). Adaptive four legged locomotion control based on nonlinear dynamical systems. In *From Animals to Animats 9. Proceedings of the Nineth International Conference on the Simulation of Adaptive Behavior (SAB 06)*.

Buchli, J., Righetti, L., and Ijspeert, A. J. (2005). A dynamical systems approach to learning: a frequency-adaptive hopper robot. In *Proceedings of the VIIIth European Conference on Artificial Life (ECAL 2005)*, Lecture Notes in Artificial Intelligence, pages 210–212.

Dürr, V., König, Y., and Kittmann, R. (2001). The antennal motor system of the stick insect *Carausius morosus*: Anatomy and antennal movement pattern during walking. *Journal of Comparative Physiology A*, 187(2):131–144.

Erber, J., Kierzek, S., Sander, E., and Grandy, K. (1998). Tactile learning in the honeybee. *Journal of Comparative Physiology A*, 183:737–744.

Esslen, J. and Kaissling, K.-E. (1976). Zahl und verteilung antennaler sensillen bei der honigbiene (*Apis mellifera* l.). *Zoomorphology*, 83:227–251. 10.1007/BF00993511.

Hochreiter, S., Bengio, Y., Frasconi, P., and Schmidhuber, J. (2001). Gradient flow in recurrent nets: the difficulty of learning long-term dependencies. In S. C. Kremer, J. F. K., editor, *A Field Guide to Dynamical Recurrent Neural Networks*. IEEE Press.

Hoinville, T., Wehner, R., and Cruse, H. (2012). Learning and retrieval of memory elements in a navigation task. In Prescott, T., Lepora, N., Mura, A., and Verschure, P., editors, *Biomimetic and Biohybrid Systems*, volume 7375 of *Lecture Notes in Computer Science*, pages 120–131. Springer Berlin Heidelberg.

Huang, G.-B., Zhu, Q.-Y., and Siew, C.-K. (2006). Extreme learning machine: Theory and applications. *Neurocomputing*, 70(1-3):489 – 501.

Ijspeert, A. J. (2008). Central pattern generators for locomotion control in animals and robots: A review. *Neural Networks*, 21(4):642 – 653.

Ijspeert, A. J., Crespi, A., Ryczko, D., and Cabelguen, J.-M. (2007). From swimming to walking with a salamander robot driven by a spinal cord model. *Science*, 315(5817):1416–1420.

Kaneko, M., Kanayama, N., and Tsuji, T. (1995). 3-d active antenna for contact sensing. In *IEEE International Conference on Robotics and Automation*, volume 1, pages 1113–1119. IEEE.

Kaneko, M., Kanayma, N., and Tsuji, T. (1998). Active antenna for contact sensing. *IEEE Transactions on Robotics and Automation*, 14(2):278–291.

Kevan, P. G. and Lane, M. A. (1985). Flower petal microtexture is a tactile cue for bees. *Proceedings of the National Academy of Sciences*, 82(14):4750–4752.

Kim, D. and Möller, R. (2007). Biomimetic whiskers for shape recognition. *Robotics and Autonomous Systems*, 55(3):229–243.

Krause, A. F. and Dürr, V. (2004). Tactile efficiency of insect antennae with two hinge joints. *Biological Cybernetics*, 91(3):168–181.

Krause, A. F. and Dürr, V. (2012). Active tactile sampling

by an insect in a step-climbing paradigm. *Frontiers in Behavioural Neuroscience*, 6(30):1–17.

Krause, A. F., Essig, K., Piefke, M., and Schack, T. (2013a). No-prop-*fast* - a high-speed multilayer neural network learning algorithm: Mnist benchmark and eye-tracking data classification. In *Engineering Applications of Neural Networks (EANN 2013)*, pages 446–455. Springer.

Krause, A. F., Winkler, A., and Dürr, V. (2013b). Central drive and proprioceptive control of antennal movements in the walking stick insect. *Journal of Physiology-Paris*, 107(1-2):116 – 129.

LeCun, Y., Bottou, L., Orr, G. B., and Müller, K.-R. (1998). Efficient backprop. In Orr, G. B. and Müller, K.-R., editors, *Neural Networks: Tricks of the Trade*, volume 1524 of *Lecture Notes in Computer Science*, pages 9–50. Springer Berlin Heidelberg.

Lederman, S. and Klatzky, R. (2009). Haptic perception: A tutorial. *Attention, Perception, & Psychophysics*, 71(7):1439–1459. 10.3758/APP.71.7.1439.

Lee, M. and Nicholls, H. (1999). Review article tactile sensing for mechatronics - a state of the art survey. *Mechatronics*, 9(1):1 – 31.

Patanè, L., Hellbach, S., Krause, A. F., Arena, P., and Dürr, V. (2012). An insect-inspired bionic sensor for tactile localization and material classification with state-dependent modulation. *Frontiers in Neurorobotics*, 6(8):1–18.

Righetti, L. and Ijspeert, A. J. (2006). Programmable central pattern generators: an application to biped locomotion control. In *IEEE International Conference on Robotics and Automation (ICRA)*, pages 1585–1590. IEEE.

Russell, R. A. and Wijaya, J. A. (2003). Object location and recognition using whisker sensors. In *Australasian Conference on Robotics and Automation*, pages 761–768.

Schilling, M., Hoinville, T., Schmitz, J., and Cruse, H. (2013). Walknet, a bio-inspired controller for hexapod walking. *Biological Cybernetics*, 107(4):397–419.

Schütz, C. and Dürr, V. (2011). Active tactile exploration for adaptive locomotion in the stick insect. *Philosophical Transactions of the Royal Society B: Biological Sciences*, 366(1581):2996–3005.

Solomon, J. H. and Hartmann, M. J. (2006). Biomechanics: Robotic whiskers used to sense features. *Nature*, 443(7111):525.

Staudacher, E., Gebhardt, M. J., and Dürr, V. (2005). Antennal movements and mechanoreception: neurobiology of active tactile sensors. *Advances in Insect Physiology*, 32:49 – 205.

Widrow, B., Greenblatt, A., Kim, Y., and Park, D. (2013). The *No-Prop* algorithm: A new learning algorithm for multilayer neural networks. *Neural Networks*, 37:182–188.